

# High fluoride in groundwater of an industrialized area of Eastern India (Odisha): inferences from geochemical and isotopic investigation

Tirumalesh Keesari<sup>1</sup>  · Uday Kumar Sinha<sup>1</sup> · Archana Deodhar<sup>1</sup> · S. H. Krishna<sup>2</sup> · Arzoo Ansari<sup>1</sup> · Hemant Mohokar<sup>1</sup> · Ashutosh Dash<sup>1</sup>

Received: 4 April 2016 / Accepted: 2 July 2016 / Published online: 19 July 2016  
© Springer-Verlag Berlin Heidelberg 2016

**Abstract** An assessment of fluoride distribution in groundwater of an industrialized area (Talchir), Odisha, India, was carried out to understand the potential sources and processes. This study is significant as the water resources are being endangered by the mining and other industrial activities in this region. High concentration of fluoride (4.4 mg/L) was observed in groundwater of this area, which was attributed mainly to mining activities. Additional source for high fluoride is the basement granitic rock containing fluoride bearing minerals like amphibole, biotite and fluorite. The dominant chemical types are found to be Na–Ca–HCO<sub>3</sub>, Na–Mg–HCO<sub>3</sub>, Ca–Mg–HCO<sub>3</sub> and Ca–Na–HCO<sub>3</sub>. The groundwater facies variation was found in accordance with the local lithology. There was no marked difference in the fluoride concentration of groundwaters between near and far off mining zone. Geochemical modeling indicated precipitation of calcite and dolomite as the driving force for the release of fluoride from the formation. In addition to the precipitation of calcite and dolomite, evapotranspiration also contributes to high fluoride in groundwater. Environmental stable isotopes inferred that there was no clear isotopic distinction between high and low fluoride groundwater and the groundwater was found to be evaporated. Environmental tritium data suggested that the groundwater was modern and fluoride enrichment was facilitated by long residence time of groundwater. Statistical methods also corroborate

the geochemical and isotopic inferences. The study highlights that natural geogenic source is the main cause for high fluoride in groundwater refuting earlier theories that attribute mining activities as the only source for high fluoride in this region.

**Keywords** Fluoride · Geogenic · Anthropogenic · Evapotranspiration · Geochemical modeling

## Introduction

Understanding the factors and processes impacting groundwater quality in aquifers is crucial for groundwater development leading to sustainable water supply. Indiscriminate exploitation of groundwater and increased inputs from anthropogenic activities pose a great threat to the groundwater resources in terms of quantity and quality. This scenario is commonly witnessed in heavily industrialized regions. Among different industries, coal based power plants impact both surface and groundwater resources through fly ash generation and waste effluent disposal into the ground respectively (Ando et al. 2001). Over 100 million tons of fly ash is produced worldwide due to combustion of coal in thermal power stations (Dhadse and Bhagia 2008) and most of this is disposed of by landfill, which contribute to environmental pollution by leaching toxic constituents such as As, Cr, Se, Pb and F that are present in several hundred parts per million (Rai 1987). It is reported that fluoride contamination of surface and groundwater is a common issue near coal fields and thermal plants (Chatterjee et al. 2008; Praharaj et al. 2003; Wang and Huang 1995), which is a cause of great concern for residents living in the vicinity of such plants. Geogenic sources also play a major role in contributing high fluoride

✉ Tirumalesh Keesari  
tirumal@barc.gov.in; tiruh2o@gmail.com

<sup>1</sup> Isotope Production and Applications Division, BARC, Mumbai, India

<sup>2</sup> Talcher Thermal Power Station, National Thermal Power Corporation, Angul, Odisha, India

levels in groundwater based on hydrochemical nature of groundwater, availability of fluoride bearing minerals, groundwater residence time, etc. The geogenic sources are diversified and complicated, mostly related to dissolution of fluoride containing minerals such as fluorite, biotite, hornblende and fluorapatite in igneous (Chae et al. 2007), metamorphic (Kundu et al. 2001) and sedimentary rocks (Kern et al. 2008). Some micas weathered from silicates, igneous and sedimentary rocks (Datta et al. 1996) and unstable minerals such as sepiolite and palygorskite also contribute fluoride to groundwater (Jacks et al. 2005; Wang and Wei 1995).

According to World Health Organization, the ill effects from drinking fluoride contaminated water are wide spread in Asian countries (Frencken 1992). There are many reports of fluoride contamination of drinking water and associated health issues in USA and UK (Ayoob and Gupta 2006), China (Qinghai Guo et al. 2007; Wang and Cheng 2001), Srilanka (Dissanayake 1991), Iran (Moghaddam and Fijani 2009; Battaleb-Looie et al. 2012a, b, 2013), Ethiopia (Rango et al. 2009) and Pakistan (Farroqi et al. 2007). In Indian context, about 60 million people are affected by fluorosis (dental, skeletal and non-skeletal) because of consumption of fluoride contaminated water (UNICEF 1999). Almost half of the Indian states have been identified as endemic areas of fluoride (Singh et al. 2013; Jacks et al. 2005; Pillai and Stanley 2002; Subba Rao 2011; Subba Rao et al. 2013 and reference therein).

Odisha State is exceptionally rich in natural resources including several strategic minerals. Availability of vast mineral deposits, abundant water supply and good infrastructure led to heavy industrialization in this state. Talcher coalfield, one of the Gondwana basins known for coal producing sector in India is also located in this state. The coal mining is carried through open cast and underground mining method and is in operation for the last few decades. The waste produced during the process of mining is dumped in open ground and the mine seepage is discharged into the cultivated lands, open area and nearby drainage system, which is being often used as source of potable water for adjoining villages (Moharana et al. 2013; Panda et al. 2010; Reza and Singh 2010). The inhabitants of this area depend on groundwater for domestic needs and consumption of poor quality groundwater has led to a number of water borne diseases (Sahu et al. 1991). Studies carried out on water quality in this region report high levels of fluoride in groundwater that is being used for drinking purposes. Most of these studies attribute the high fluoride concentration in groundwaters to the contribution of wastes from power plant activities (Deshmukh et al. 1995; Moharana et al. 2013; Nanda et al. 2011; Panda et al. 2010; Reza and Singh 2010; Dhakate and Rao 2010) but no clear evidences were presented. Few authors also opined that

weathering and erosion of bed rocks might also cause high fluoride in groundwater (Moharana et al. 2013; Reza and Singh 2010), but no scientific data was presented in this regard. Most of the studies dealing with the water quality of this region has emphasized the need to pre-treat the water before being used for drinking purposes.

In spite of several reports on occurrence of high fluoride in groundwaters of this region, there were no detailed studies on the geochemistry of groundwater and factors leading to high fluoride in groundwater of this region. Since drinking high fluoride groundwater is the major reason for endemic fluorosis and has considerable impact on human health, it becomes imperative to examine the sources of fluoride in groundwater of this region so that amelioration methods can be adopted to mitigate the groundwater contamination. In the present study, an environmental isotopic and geochemical investigation was carried out to (i) assess the water quality; (ii) evaluate geochemical processes governing fluoride release into groundwater of Talcher region.

## Study area description

### Location

The study region belongs to Angul District of Odisha state, which is located on the right bank of the River Brahmani. The geographical coordinates of the study area are; latitude  $20^{\circ}52'30''$  and  $20^{\circ}57'30''$  and longitude  $85^{\circ}08'30''$  and  $85^{\circ}14'30''$ . The total geographical area is about  $150 \text{ km}^2$  and the mean elevation is 140 m above sea level. Angul district can be broadly divided into three major physiographic units, (1) northern mountainous region, (2) central undulating plain and (3) southern and southwestern mountainous region.

### Geology

This region represents a diverse geological sequence, from rocks of Eastern Ghats of Pre-Cambrian age, Iron-ore super group, Gondwana Super group, Laterites to alluvial deposits of Quaternary age (Manjrekar et al. 1998). The geological succession is given in Table 1.

The main lithological units of this area are dominantly glaciogenic sediments that were accumulated within shallow erosional embryonic basins amidst Archean basement. These units are typically mica, schist, phyllite and amphibolites, sandstones and greenish needle shales.

### Hydrogeology

The groundwater occurrence and distribution in space and time is highly controlled by geomorphology of the study

**Table 1** Stratigraphic units of study area

Age	Formation	Lithology
Recent		Alluvium and Laterite
Upper Permian to Triassic	Kamathi	Fine to medium grained sandstone, carbonaceous shale, coal bands, with greenish, pink clays and pebbly sandstones at top
Lower Permian (Gondwana Supergroup)	Barakar	Medium to coarse grained sandstone, shales, coal seam with oligomictic conglomerate at base
	Karharbari	Medium to coarse grained sandstone, shales, coal seams
	Talchir	Diamictite, fine to medium grained greenish sandstones, shales, rhythmite, turbidite etc.
Unconformity		
Precambrian		Granite, gneisses, amphibolites, migmatites, etc.

area. Bore wells, hand pumps and dug wells are commonly used for groundwater extraction in both Crystalline and Gondwana rocks in this region. Groundwater occurs under water table condition in weathered formation and under semi confined to confined condition in fractured zones of the underlying formations. The bore wells drilled up to 200 m depth have limited yield varying from 2 to 5 Lps depending on the fractures encountered.

The average depth of dug wells is about 10 m bgl while in Gondwana formation the depth of wells is up to 300 m bgl. The depth of water level during pre- monsoon period ranges from 1.26 to 13.69 m bgl and during post-monsoon it ranges from 0.60 to 12.52 m bgl (Tiwary et al. 2009). The water table elevation in the area generally follows the topography and the general groundwater flow is from North East to South West directed towards river Brahmani (Dhakate et al. 2013). The study area is characterized by three distinct seasons viz., winter (November to February), summer (March to June) and rainy (June and September). The two major rivers namely Mahanadi and Brahmani are flowing on the two sides of the study area. The Mahanadi river flows toward ESE forming SW boundary, while the Brahmani flows toward SE. These two rivers along with their tributaries form the drainage system in this region. The average annual rainfall in the district is 1400 mm.

**Sampling and measurements**

A total of 32 samples including groundwater (27), river (2) and rainwater (3) were collected. Groundwaters were mainly collected from hand pumps covering quarries and fly ash dumps, while surface waters were collected from nearby rivers. Sample locations along with rivers, quarries and ash ponds are shown in Fig. 1. Water samples were filtered using 0.45µm pore size membrane filters and stored in clean polyethylene bottles. Another set was

collected and acidified to pH 2 by adding ultra pure concentrated HNO<sub>3</sub> for cation measurements. Physical parameters like pH, temperature, dissolved oxygen (DO), and electrical conductivity (EC) were measured in situ. DO and pH readings were obtained by Corning (model 313) and, temperature and conductivity by Orion meter (model 130). Alkalinity was measured in the field by titrating 10 mL of water sample with 0.02 N H<sub>2</sub>SO<sub>4</sub>. A mixed indicator (Bromocresol green–Methyl red) was used to mark the end point. Alkalinity (in mg CaCO<sub>3</sub>/L) was multiplied by a factor of 1.22 to obtain HCO<sub>3</sub><sup>-</sup> concentration (in mg/L).

Anions viz., Cl<sup>-</sup>, SO<sub>4</sub><sup>2-</sup>, NO<sub>3</sub><sup>-</sup> and F<sup>-</sup> and cations viz., Na<sup>+</sup>, Ca<sup>2+</sup>, Mg<sup>2+</sup>, K<sup>+</sup> and Li<sup>+</sup> were analyzed using ion chromatography (Dionex, DX-500) employing electrochemical detector (ED 40) in conductivity mode. The separation of anions was performed through an anion exchanging column (Ion Pack AS-11) and the elution was carried out by dilute sodium hydroxide while for cations the separating column used was Ion Pack CS-12A and elution was performed by dilute sulfuric acid. The flow rate of eluant was 1 mL/min and the volume of the water sample injected was 25 µL. Hydrochemical data is listed in Table 2. The accuracy of the chemical ion data was calculated using charge balance equation given below and the charge balance error (CBE) values of majority of the samples were within the accepted limits of ±5 % (Hounslow 1995).

$$CBE (\%) = \frac{meq(cations) - meq(anions)}{meq(cations) + meq(anions)} \times 100 \quad (1)$$

For stable isotope (<sup>2</sup>H and <sup>18</sup>O) analysis, water samples were collected in 50 mL airtight high density polyethylene bottles and measured by continuous flow Isotope Ratio Mass Spectrometer (Isoprime 100). For δ<sup>2</sup>H analysis, 1 mL of the water sample was equilibrated with H<sub>2</sub> in presence of Pt-coated Hokko beads catalyst at 50 °C for 90 min and the gas was introduced into the mass spectrometer (Ohsumi

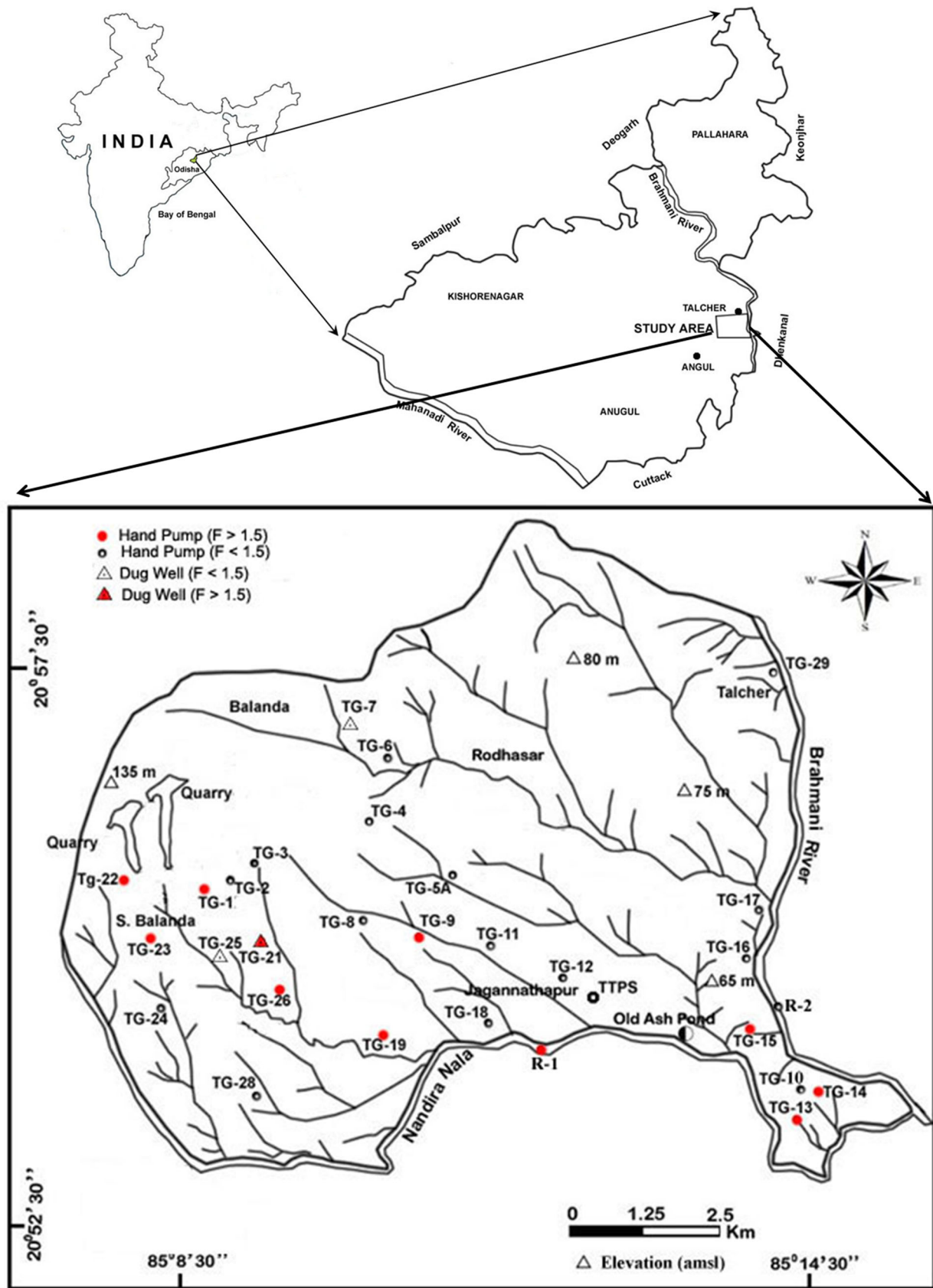


Fig. 1 Location map of the study area with sampling points

**Table 2** Physico-chemical, environmental isotopes data of water samples, Talchir area

Sample ID	Source	T (°C)	pH	EC (µs/cm)	TDS (mg/L)	DO (mg/L)	Li <sup>+</sup> (mg/L)	Na <sup>+</sup> (mg/L)	K <sup>+</sup> (mg/L)	Mg <sup>2+</sup> (mg/L)
TG-1	HP	29.4	7	1545	1081	4.35				
TG-2	HP	29.2	6.4	183	129	5.67	0.02	16.4	5	4.7
TG-3	HP	29.1	6.3	253	178	6.08	0.01			
TG-4	HP	29.7	6.8	614	430	4.64		65	6.6	21.7
TG-5	HP	28.6	6.7	1852	1297	5.05				
TG-6	HP	28.8	7.1	352	256	5.6		21.3	12.1	7.3
TG-7	DW	28.8	7.3	450	317	5.81				
TG-8	HP	29.3	7.5	800	561	4.9		63.5	15.3	57.2
TG-9	HP	29.7	7.5	817	572	5.26		117	4.6	56.5
TG-11	HP	29.5	7	1257	878	5.17	0.02	139	1.3	28.4
TG-12	HP	28.9	6.4	1291	903	5.28		123	1.5	23
TG-13	HP	29.9	7.4	996	696	4.28		137	0.67	6.7
TG-14	HP	29.8	7.1	960	672	4.4	0.02	73.5	2.1	18.4
TG-14A	HP	29.6	7.1	377	264	4.18		53.8		39
TG-15	HP	30.7	7.1	1508	1056	4.81		102		19.6
TG-16	HP	29.1	7.4	579	406	7.4		16.9	0.9	12.1
TG-17	HP	30.4	7.6	709	496	6.8		59.6	0.64	26
TG-18	HP	29.3	7.2	1910	1340	4.75	0.02	119	15.1	28.7
TG-19	HP	28.8	7.6	2160	1510	6.45		316	3.2	108
TG-21	DW	27.76	7.61	674	472	4.97		53	1	26
TG-22	HP	29.6	6.6	306	215	5.45				
TG-23	HP	29.2	7.6	1061	744	4.29		191	1.6	40
TG-24	HP	29.2	7.1	1411	987	5.17		16.6	4.3	2.9
TG-25	DW	26.8	7.8	1515	1061	5.3		168	4.2	14.3
TG-26	HP	28.1	7.2	2195	1534	4.89		161	4.9	83.5
TG-28	HP	29.1	7.1	1956	1371	4.77		37.5	7.9	54
TG-29	HP	29.7	7	287	202	5.22				
R-1	Surface	29.5	7.4	145	66	6.9		6.5	2	3.3
R-2	Surface	25	8.6	512	291	8.42	0.08	34.1	3.9	15.8
Rain-1	Rain							0.56	0.28	0.3
Rain-2	Rain							0.23	0.19	0.05
Rain-3	Rain							0.3	0.17	0.19
Average <sup>a</sup>		29.19	7.13	1037.70	726.96	5.22	0.02	97.62	4.89	32.29
Sample ID	Ca <sup>2+</sup> (mg/L)	F <sup>-</sup> (mg/L)	Cl <sup>-</sup> (mg/L)	NO <sub>3</sub> <sup>-</sup> (mg/L)	SO <sub>4</sub> <sup>2-</sup> (mg/L)	HCO <sub>3</sub> <sup>-</sup> (mg/L)	δ <sup>2</sup> H (‰)	δ <sup>18</sup> O (‰)	<sup>3</sup> H (T.U.)	
TG-1		1.7	229	6.2	95.4	363.5	-18.33	-3.26		
TG-2	24	0.13	7.14	1.6	2.8	146.4	-30.05	-5.07		
TG-3		0.8	54.3	4.5	10.1	44	-33.84	-5.23		
TG-4	51.5	0.15	25	2.3	25	295.2	-28.65	-4.55		
TG-5		1.2	507	147	207	354	-24.37	-3.62	3.42	
TG-6	18.3	0.8	21.1	3	1.2	133	-33.26	-4.32		
TG-7		0.32	27.6	18.4	52.8	313.5	-33.14	-4.6		
TG-8	97	0.4	53	27	82	500	-32.12	-4.78		
TG-9	58.5	1.8	136	27	59	318.4	-23.29	-3.54		
TG-11	14.9	1.4	17.8	0.9	13.7	450.2	-20.8	-3.78		
TG-12	99	1.1	149	28.5	105	465	-20.84	-3.23		
TG-13	25.9	4.4	35.1	0.5	14.5	475.8	-22.44	-3.23	3.3	
TG-14	55.5	1.8	23.7	1	13.9	352.5	-32.28	-4.54		

**Table 2** continued

Sample ID	Ca <sup>2+</sup> (mg/L)	F <sup>-</sup> (mg/L)	Cl <sup>-</sup> (mg/L)	NO <sub>3</sub> <sup>-</sup> (mg/L)	SO <sub>4</sub> <sup>2-</sup> (mg/L)	HCO <sub>3</sub> <sup>-</sup> (mg/L)	δ <sup>2</sup> H (‰)	δ <sup>18</sup> O (‰)	<sup>3</sup> H (T.U.)
TG-14A	121	0.75	61.5	67.6	61.9	380	-30.31	-4.43	
TG-15	30.3	1.7	37.9	3.9	12.4	447.7	-27.36	-4.33	1.92
TG-16	45.5	0.4	11	19	12.5	220	-23.34	-3.21	
TG-17	97.8	0.48	40	11.7	28.6	470.9	-25.35	-3.74	
TG-18	102	1.3	139	4.7	73.5	399	-22.54	-3.54	
TG-19	91	3.7	685	26	174	78.8	-27.62	-2.8	1.73
TG-21	25	1.5	35	20.4	66	240	-22	-3.04	
TG-22		1.7	346	33.8	199	190	-29.34	-4.43	2.2
TG-23	20.9	1.5	76.7	29.7	88	632	-19.57	-2.84	
TG-24	24	0.3	14.5	4.8	13.6	114.2	-19.82	-2.34	
TG-25	64.5	0.5	113	38.7	118	405	-27.25	-4.27	
TG-26	114	1.6	195	81	127	527	-30.77	-3.1	
TG-28	96.4	1.1	217	43	51	248	-22.12	-3.66	
TG-29		0.9	15	8.2	13	163.5	-28.68	-4.92	
R-1	11.6	1.8	8	1	5	58.3	-37.36	-5.55	4.2
R-2	61.1	1.4	18	1.5	52	219.6	-27.8	-3.61	
Rain-1	3.6	0.08	5	0	5	16.4	-35.7	-5.22	3.5
Rain-2	2.8	0.21	36	0	21	10.5	-36.1	-5.4	5
Rain-3	3.2	0.4	48	0	19	16.5	-36.7	-5.21	4.2
Average <sup>a</sup>	60.81	1.24	121.20	24.46	63.74	323.24	-26.28	-3.87	2.51

HP, hand pump; DW, dug well; R-1, Brahmani River; R-2, Nandira Nala

<sup>a</sup> Average of groundwater samples only

and Fujino 1986). The δ<sup>18</sup>O of the sample was measured by equilibrating 1 mL of water with CO<sub>2</sub> gas at 50 °C for 8 h and the equilibrated gas was introduced into the mass spectrometer (Epstein and Mayeda 1953; Horita et al. 1989). The results are reported in δ-notation and expressed in units of parts per thousand (denoted as ‰). The δ values are calculated using (Coplen 1996):

$$\delta(\text{‰}) = \left( \frac{R_x}{R_s} - 1 \right) \times 1000 \quad (2)$$

where  $R$  denotes the ratio of heavy to light isotope (e.g., <sup>2</sup>H/<sup>1</sup>H or <sup>18</sup>O/<sup>16</sup>O) and  $R_x$  and  $R_s$  are the ratios in the sample and standard, respectively. The measured values are normalized on VSMOW/SLAP scale as per the methodology established by Nelson (2000). The precision of measurement for δ<sup>2</sup>H is ±0.5 ‰ and for δ<sup>18</sup>O is ±0.1 ‰ (2σ).

The tritium content of the water samples was measured by a liquid scintillation counter (Perkin Elmer Quantulus-Model No. 1220) proceeded by electrolytic enrichment (Nair 1983). Tritium concentration is expressed in tritium unit (TU), where 1 TU corresponds to one tritium atom per 10<sup>18</sup> protium atoms. The precision of the measurement is ±0.5 TU (2σ). The hydrochemical data along with environmental isotopes is presented in Table 2.

## Results and discussion

### General water quality

Temperature of the groundwater in this area varies from 26.8 to 30.7 °C with a narrow distribution around an average of 29.2 ± 0.8 °C (Table 2). The pH values in groundwaters of this area range from 6.3 to 7.8 with an average of 7.13 (Table 2). Groundwaters are found to be slightly acidic to slightly alkaline in nature. Samples collected from both rivers show neutral to alkaline pH (7.4 to 8.6). Samples with acidic pH (<6.5) are generally located on the western part of the study area. Only one sample (Nandira Nala) showed alkaline pH (8.6). The groundwater samples have EC in the range 183–2195 μS/cm with an average of 1038 ± 628 μS/cm (Table 2). The high EC values (~2000 μS/cm) are noted in only four samples (TG-18, 19, 26 and 28), which are located down-stream of quarries in the western part of the study area. The water samples collected in the study area show DO between 4.2 and 7.4 mg/L with an average value of 5.2 ± 0.8 mg/L (Table 2). River waters show high DO in the range of 6.9–8.6 mg/L. No systematic spatial variation in DO concentration is observed in the study area. The DO results indicate that groundwater is in equilibrium with the

atmosphere, suggesting that the recharge is modern which is further confirmed by environmental tritium data (“[Environmental isotopic characteristics](#)” section).

The Na<sup>+</sup> concentration in groundwater ranges from 15 to 316 mg/L with a wide distribution around a mean value of 98 ± 74 mg/L (Table 2). Higher Na<sup>+</sup> values are noted in TG-19 (316 mg/L) and TG-23 (191 mg/L), which are close to Nandira Nala and quarry, respectively. Dissolution of alkali feldspar minerals, ion exchange processes, sewage contamination and infiltration from agricultural runoff are common sources of Na<sup>+</sup> concentration in groundwater. Potassium concentration in groundwater of this region varies from 0.6 to 15.3 mg/L with a mean value of 4.9 ± 4.4 mg/L (Table 2). Clay minerals present in the study area can be potential sources for potassium. The concentration of Mg<sup>2+</sup> in groundwater of this region varies from 3 to 108 mg/L, and the mean is 32 ± 26 mg/L (Table 2). The potential source of Mg<sup>2+</sup> is mainly carbonate and biotite minerals present in the study area. Ca<sup>2+</sup> concentration in groundwater of this region ranges from 12.1 to 121 mg/L with a mean value of 61 ± 36 mg/L (Table 2). Ca<sup>2+</sup> in natural water is mainly contributed by sulfate, carbonate minerals and plagioclase feldspar.

Chloride is one of the main anions present in natural waters. High concentrations of Cl<sup>-</sup> in natural water may result from contamination by sewage, seawater and saline residues in the soil (Hem 1985). Chloride concentration in groundwater ranges from 7 to 685 mg/L with a wide variation around a mean of 121 ± 162 mg/L (Table 2). Dissolution of minerals and sewage contribution are the main sources of Cl<sup>-</sup> in groundwaters of this region. Nitrate being soluble and mobile is prone to leaching through soils with infiltrating water. Decaying organic matter, domestic wastes (David and Gentry 2000) and fertilizers (Tripathi et al. 2000) are major sources of nitrate in groundwater. The nitrate concentration in groundwater of this area ranges from 0.5 to 147 mg/L with a mean value of 24.5 ± 32 mg/L (Table 2). Three samples (TG-5, TG-14A and TG-26) show high nitrate concentration above drinking water permissible limit of 50 mg/L (WHO 2011). Sewage and agricultural contributions are the main reasons for nitrate in this region. Sulfate concentration in study area

shows a wide variation from 1 to 207 mg/L with a mean of 64 ± 60 mg/L (Table 2). Wastes resulting from domestic activities, feedlots and agricultural runoff also add excess SO<sub>4</sub><sup>2-</sup> concentration to groundwater. The presence of bicarbonate (HCO<sub>3</sub><sup>-</sup>) is mostly responsible for alkalinity of groundwater, and it ranges from 44 to 632 mg/L with a mean value of 323 ± 154 mg/L (Table 2). The alkalinity in groundwater is mainly contributed by root respiration as well as carbonate mineral dissolution.

### Fluoride distribution

The F<sup>-</sup> concentration in the study is found in the range of 0.13 to 4.4 mg/L with an average of 1.2 ± 1.0 mg/L. About 37 % of the samples measured show F<sup>-</sup> concentration above the WHO guideline value of 1.5 mg/L (WHO 2011). Rain water and a few groundwater samples show F<sup>-</sup> concentration less than 0.5 mg/L, whereas both the surface water samples show F<sup>-</sup> concentration close to 1.5 mg/L. The percentage of samples falling in different categories based on F<sup>-</sup> effect on human health (compiled after Subba Rao et al. 2013) is given in Table 3.

From Table 3, it is evident that about 48 % of the groundwater samples can lead to detrimental effects upon consumption for drinking purposes. Researchers have reported high fluoride content up to 2.8 mg/L in groundwater of this area (Moharana et al. 2013), and the possible reason ascribed was contribution from the effluents from thermal power station. Similarly other researchers reported that groundwater especially in shallow zone is vulnerable to fluoride contamination (Deshmukh et al. 1995; Reza and Singh 2010). It is found that groundwater samples with fluoride level higher than 1.5 mg/L are all scattered throughout the study area (Fig. 1). Groundwater with F > 1.5 mg/L is found to fall downstream of the quarries (TG-1, 21, 22, 23, 25, 26 and 28) and near the confluence point of the River and Nala (TG-13, 14 and 15). One sample (TG-9) located in the central part of the study area also shows F<sup>-</sup> > 1.5 mg/L. Fluoride occurrence in groundwater located close to the thermal plant site does not show any remarkable enrichment compared to far away

**Table 3** Percent fluoride distribution and the related health effects

Fluoride concentration (mg/L)	Percentage of samples	Health Effects
<0.6	29.63	Dental caries
0.6–1.2	22.22	Development of normal bones and teeth
1.2–2.0	40.74	Mottled enamel
2.0–4.0	3.70	Dental fluorosis
4.0–8.0	3.70	Skeletal fluorosis
8.0–10.0	0.00	Mild crippling skeletal fluorosis
>10	0.00	Crippling skeletal fluorosis

**Fig. 2** Bar chart of average values of **a** major ions and **b** environmental isotopes in groundwater with different fluoride concentrations

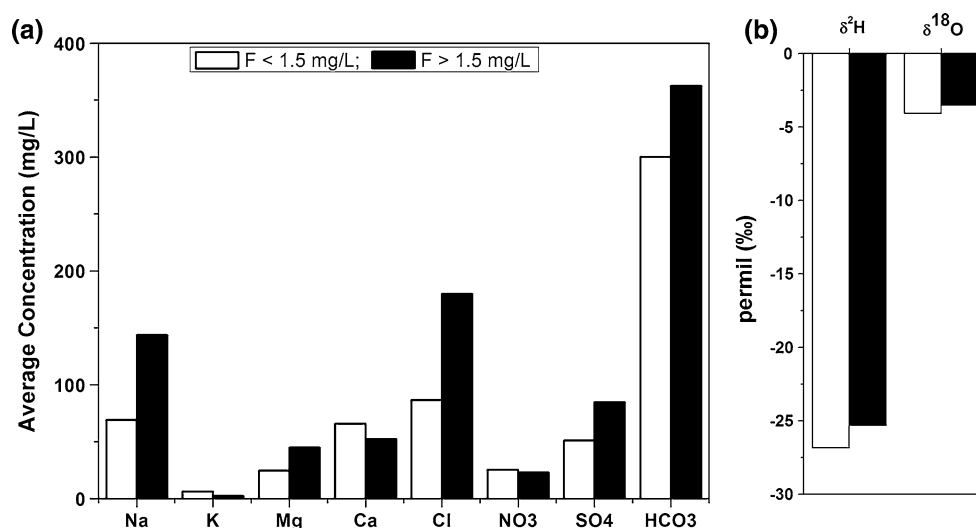
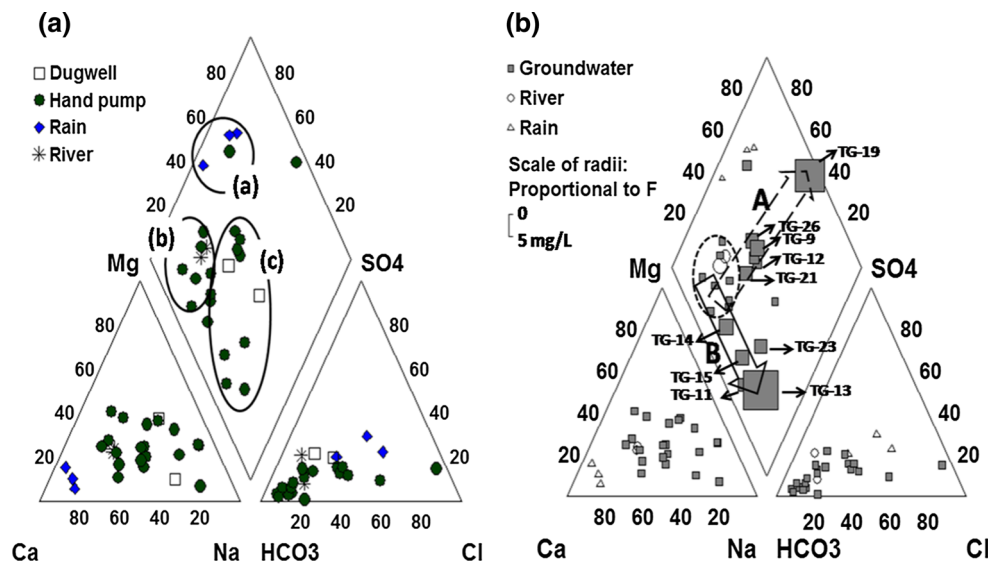


**Fig. 3** Piper's trilinear plot depicting **a** rock dominance of groundwater and **b** geochemical pathways of groundwater facies evolution



sites. This suggests that thermal power plant effluents are not the only sources for high fluoride observed in groundwater of this area as pointed out by the earlier researchers (Nanda et al. 2011; Panda et al. 2010; Reza et al. 2009).

### Geochemical evolution of groundwaters

The  $F^-$  concentration is largely controlled by groundwater chemistry. Higher total dissolved solids can aid in enhancing  $F^-$  concentration in groundwater (Jacks et al. 1993; Keesari et al. 2007). It can be seen from the Fig. 2a that the average values of other major ions in high  $F^-$  groundwater ( $F^- > 1.5 \text{ mg/L}$ ) are higher than those in low  $F^-$  groundwater ( $F^- < 1.5 \text{ mg/L}$ ).  $Ca^{2+}$  and to some extent  $K^+$  and  $NO_3^-$  show opposite trends.

Further, geochemical interpretation was carried out using Piper's trilinear plot in order to find out variation in chemical facies and the geochemical evolution of groundwater. All the samples show  $Na^+$  and  $Ca^{2+}$  as dominant cations, while  $Mg^{2+}$  is found in low concentration.  $HCO_3^-$  and  $Cl^-$  are the dominant anions, while  $SO_4^{2-}$  is present in relatively low concentration. Groundwater shows four major chemical types, viz., Na–Ca– $HCO_3$ , Na–Mg– $HCO_3$ , Ca–Mg– $HCO_3$  and Ca–Na– $HCO_3$ . A few representations of Na–Mg–Cl and Na– $HCO_3$  are also observed. Rain waters are predominantly Ca–Cl– $HCO_3$ , while river waters are Ca–Na– $HCO_3$  types. Piper plot was also used to relate the water composition to the rock types from which the water was extracted based on the classification by Zuurdeeg and Van der weiden (1985). It is observed from the Fig. 3a that the facies variation follows



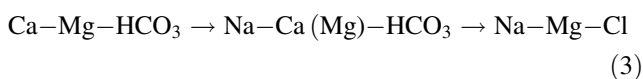
**Table 4** Mineral saturation indices, base exchange indices and characteristic ionic ratio of water samples

Sample ID	Magnesite	Calcite	Gypsum	Fluorite	Dolomite	CAI-1	CAI-2	Cl <sup>-</sup> /∑ anions
TG-1								0.44
TG-2	-2.30	-1.40	-3.48	-3.21	-3.11	-3.18	-0.26	0.07
TG-3								0.60
TG-4	-1.02	-0.45	-2.37	-2.89	-0.88	-3.25	-0.42	0.12
TG-5								0.53
TG-6	-10.26	-9.17	-6.32		-18.97	-1.08	-0.28	0.21
TG-7								0.11
TG-8	0.23	0.65	-1.75		1.47	-1.11	-0.16	0.13
TG-9	0.07	0.27	-2.06	-1.90	0.93	-0.36	-0.20	0.36
TG-11	-0.54	-0.63	-3.19	-2.26	-0.58	-11.12	-0.73	0.06
TG-12	-1.30	-0.47	-1.60	-0.97	-1.18	-0.28	-0.12	0.29
TG-13	-0.74	0.04	-2.90	-0.26	-0.11	-5.04	-0.61	0.11
TG-14	-0.72	-0.05	-2.60	-0.93	-0.18	-3.87	-0.42	0.10
TG-14A	-0.42	0.26	-1.74	-1.22	0.43	-0.35	-0.07	0.17
TG-15	-0.58	-0.21	-2.92	-1.05	-0.19	-3.15	-0.44	0.12
TG-16	-0.77	0.00	-2.65	-2.03	-0.18	-1.45	-0.11	0.07
TG-17	0.02	0.78	-2.13	-1.68	1.39	-1.31	-0.17	0.12
TG-18	-0.45	0.29	-1.74	-0.81	0.43	-0.42	-0.20	0.32
TG-19	-1.26	-1.13	-1.56	-0.10	-1.80	0.28	1.03	0.78
TG-21	0.12	0.17	-2.13		0.87	-1.36	-0.24	0.15
TG-22							0.00	0.56
TG-23	0.27	0.18	-2.35		1.03	-2.86	-0.49	0.15
TG-24	-1.92	-0.81	-2.78		-2.14	-1.04	-0.19	0.15
TG-25	-0.21	0.66	-1.69		1.03	-1.33	-0.43	0.25
TG-26	0.05	0.39	-1.57	-0.69	1.02	-0.30	-0.13	0.30
TG-28	-0.53	-0.06	-1.94	-1.01	0.00	0.70	0.74	0.51
TG-29							0.00	0.12

closely with the lithology of this region. Group (a) samples fall in the field of rainwater, Ca–Cl–HCO<sub>3</sub>–SO<sub>4</sub>, which are influenced by the local atmospheric dust. Group (b) samples fall in carbonate rock type (Ca–Mg–HCO<sub>3</sub>) and group (c) samples fall in shale, sandstone, granitic rock types (Na–Ca–HCO<sub>3</sub>, Na–Ca–HCO<sub>3</sub>–Cl and Na–Mg–HCO<sub>3</sub>–Cl). The facies variation is found to be in good agreement with the geology comprising of Precambrian rocks (granite and gneisses), Talchir formation (sandstone and shale) and carbonate minerals in the region (Bhattacharya et al. 2002; Dasgupta 2006).

A close look at the facies change in diamond field of Piper’s plot (Fig. 3b) infers two geochemical pathways; A and B.

In pathway A, the groundwater changes its facies as follows;



Groundwater starts as Ca–Mg–HCO<sub>3</sub> facies and changes to Na–Ca(Mg)–HCO<sub>3</sub> by accumulating the salts from the

formation either by dissolution or leaching and finally attains Na–Mg–Cl composition. The facies variation in groundwater shown above follows the normally observed geochemical evolution (Chebotarev 1955). In addition, it can also be possible that ion exchange may modify the chemical composition of the groundwater depending on its interaction with clay in the subsurface. The ion exchange process is verified by examining the base exchange indices (CAI 1 and CAI 2) as given by (Schoeller 1967);

$$\text{CAI 1} = \frac{\text{Cl}^- - \text{Na}^+ - \text{K}^+}{\text{Cl}^-} \tag{4}$$

$$\text{CAI 2} = \frac{\text{Cl}^- - \text{Na}^+ + \text{K}^+}{\text{SO}_4^{2-} + \text{HCO}_3^- + \text{CO}_3^{2-} + \text{NO}_3^-} \tag{5}$$

The concentrations are expressed in milliequivalents. If ion exchange process occurs between the dissolved Na<sup>+</sup> and K<sup>+</sup> in the water and the adsorbed Mg<sup>2+</sup> and Ca<sup>2+</sup> in the clay matrix, both of the indices are expected to be positive. However, if the exchange occurs in the reverse order, then the indices are negative. From Table 4, it can be noted that both the indices are negative in majority of the

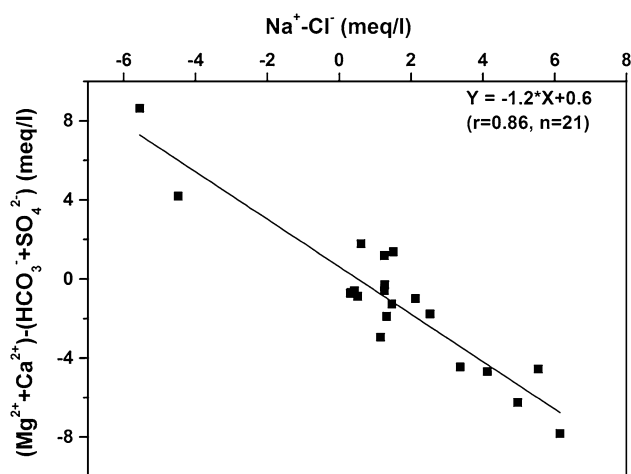
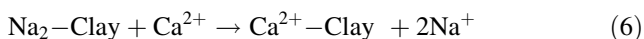


**Fig. 4** Plot of  $(\text{Ca}^{2+} + \text{Mg}^{2+}) - (\text{HCO}_3^- + \text{SO}_4^{2-})$  versus  $\text{Na}^+ - \text{Cl}^-$  to demonstrate ion exchanging process

cases, except in two samples (TG-19 and 28). Hence, the governing ion exchange reaction can be written as follows;



The ion exchange process occurring in the groundwater is further verified by  $(\text{Ca}^{2+} + \text{Mg}^{2+}) - (\text{HCO}_3^- + \text{SO}_4^{2-})$  versus  $\text{Na}^+ - \text{Cl}^-$  (milliequivalents per liter) plot. Water undergoing ion exchange would fall on a line with slope of  $-1$ , while water plotting close to the zero value on the  $x$ -axis is not influenced by ion exchange (Jankowski et al. 1998). Figure 4 shows that the slope of the best fit equation is close to  $-1$  (slope  $-1.2$ ) confirming the ion exchange process.

It is observed that the  $\text{F}^-$  content of the samples increases from initial to final stage of geochemical evolution of groundwater (Fig. 3b, line A). Water sample of TG-19 is found to contain very high  $\text{F}^-$  content (3.7 mg/L) and shows Na–Mg–Cl water type. This sample also falls on the downstream of the groundwater flow. The geochemical process governing the accumulation of  $\text{F}^-$  in groundwater seems to be interaction of groundwater with rocks containing fluoride bearing minerals. In order to further confirm this hypothesis,  $\text{F}^-/\text{Cl}^-$  (molar ratio) versus  $\text{F}^-$  concentration of the groundwater was plotted (Fig. 5). The molar ratio of  $\text{F}^-/\text{Cl}^-$  in groundwater varies between 0.004 and 0.23 with an average of 0.05. From the plot it can be observed that samples fall in two different trend lines A and B (Fig. 5). Samples falling on trend line A show higher  $\text{F}^-/\text{Cl}^-$  molar ratio ranging from 0.06 to 0.23 and also show a positive correlation between  $\text{F}^-/\text{Cl}^-$  molar ratio and corresponding  $\text{F}^-$  concentration (Fig. 5, line A). It is observed that the samples falling on trend line A also show facies change as per the pathway A shown in Piper's plot (Fig. 3b, line A). Therefore, it can be inferred that dissolution or leaching of fluoride bearing minerals is a major process

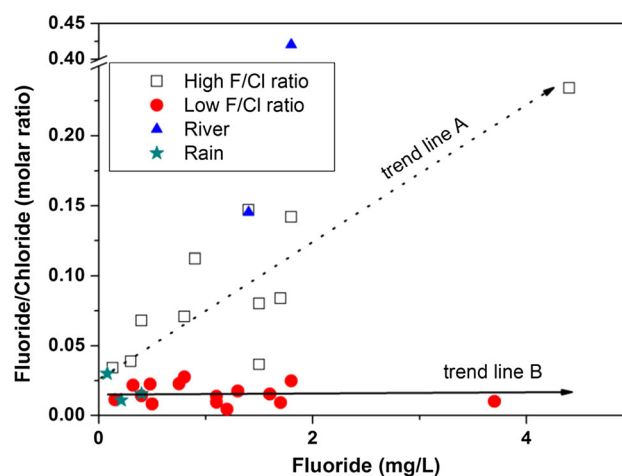
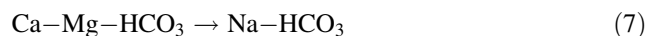


**Fig. 5** Scatter plot of  $\text{F}^-$  versus  $\text{F}^-/\text{Cl}^-$  molar ratio depicting the rock weathering (dotted trend line A) and evaporation processes (solid trend line B)

controlling the  $\text{F}^-$  distribution in groundwaters of this region. The plausible reactions and minerals responsible for the release of  $\text{F}^-$  from aquifer matrix to groundwater are discussed in “[Fluoride release mechanism](#)” section.

In pathway B, the groundwater changes its facies as follows;



The initial composition of groundwater is Ca–Mg– $\text{HCO}_3$  type, and it changes to Na– $\text{HCO}_3$ . Majority of the groundwater samples falling in this pathway show Na– $\text{HCO}_3$  type water with a very few representations from Na–Ca(Mg)– $\text{HCO}_3$  type. The variation from Ca-dominant type to Na-dominant type in the groundwater could be due to calcite precipitation or ion exchange. From the earlier discussion (pathway A), it can be found that ion exchange is the most likely mechanism. However, since this area falls under semi-arid, evaporation process can lead to calcite precipitation, which may also contribute to facies variation from Ca type to Na type. The saturation index values for calcite mineral also indicate supersaturation (Table 4), pointing to possibility of calcite precipitation being the cause for the observed facies variation. Further discussion on saturation indices of minerals is presented in “[Fluoride release mechanism](#)” section.

The highest fluoride content noticed in this pathway is 4.4 mg/L (TG-13). The fluoride concentration increases from the initial to final stages of the groundwater evolution in this pathway as well (Fig. 3b, line B). Since there is no significant variation in geochemical characteristics of the subsequent groundwaters falling in this pathway, it appears that the fluoride enrichment in groundwater is mostly governed by evapotranspiration. Similar relationship between evaporation and fluoride enrichment was noticed

by Datta et al. (1996) at Rajasthan and Keesari et al. (2007) at Karnataka (India), where strong evapotranspiration was attributed to the occurrence of high F<sup>-</sup> content in the groundwater. Although evapotranspiration is favorable for F<sup>-</sup> enrichment in groundwater, F<sup>-</sup> in groundwater cannot be enriched infinitely with excessive evapotranspiration due to formation of secondary salts (CaF<sub>2</sub> or MgF<sub>2</sub>). This region falls under semi-arid and also experiences hot climate; hence, evapotranspiration contribution to the occurrence of high F<sup>-</sup> concentration in groundwater cannot be ruled out, particularly in the wells with shallow depths.

The evaporation hypothesis is further verified from F<sup>-</sup>/Cl<sup>-</sup> versus F<sup>-</sup> plot (Fig. 5). During evapotranspiration, the F<sup>-</sup> being contributed by rainwater gets concentrated in the unsaturated zone, while it percolates and reaches water table. This process leads to elevated F<sup>-</sup> levels keeping a constant F<sup>-</sup>/Cl<sup>-</sup> molar ratio. It is found that the samples falling in geochemical pathway B exhibit low F<sup>-</sup>/Cl<sup>-</sup> molar ratio. There is no change in the F<sup>-</sup>/Cl<sup>-</sup> molar ratio with increasing fluoride concentration (Fig. 5, solid line B). The mean of the F<sup>-</sup>/Cl<sup>-</sup> is found to be 0.015, which is close to the unpolluted rainwater composition of 0.02 as reported by Saether et al. (1995). Rainwater samples collected in this region during monsoon period show F<sup>-</sup>/Cl<sup>-</sup> molar ratio equal to or less than 0.025, indicating that the fluoride in rainwater is not significantly high even though this region is highly industrialized. It is reported by many researchers that industrial emissions lead to considerably high amount of fluoride in dry and wet depositions (Chaurasia and Mishra 2007). Das et al. (1981) reported 0.1 mg/L of fluoride in rainfall of Bhopal (India). In other studies, F<sup>-</sup> concentration in rainwater was found to be ranging from 0.05 to 0.3 mg/L in central parts of India and the source was attributed to soil dust (Chandrawanshi and Patel 1999; Satsangi et al. 1998; Singh et al. 2001). Even in the places that are not industrialized, the atmospheric deposition of F<sup>-</sup> can be considerable and thought to be derived from crustal sources or marine aerosols (Satsangi et al. 2002). In similar way, the F<sup>-</sup> levels in the rain samples of the study area are in the range of 0.08 to 0.2 mg/L with low F<sup>-</sup>/Cl<sup>-</sup> molar ratios. The surface water samples show that the F<sup>-</sup> levels are close to 1.5 mg/L with higher F<sup>-</sup>/Cl<sup>-</sup> molar ratios (0.15 – 0.4), which could be due to dumping of industrial wastes at these locations. Similar levels of F<sup>-</sup> concentrations were reported in surface waters of this area in study conducted by Reza and Singh (2013).

**Environmental isotopic characteristics**

The two processes (evapotranspiration and rock weathering) controlling the fluoride enrichment in groundwater are further evaluated by isotope techniques. Hydrogen and

oxygen isotopes of water can be potential tracers to understand the effect of evaporation on the groundwater system (Clark and Fritz 1997; Craig et al. 1963). Environmental isotopes (<sup>2</sup>H, <sup>3</sup>H, <sup>13</sup>C, <sup>14</sup>C, <sup>15</sup>N, <sup>18</sup>O, <sup>34</sup>S and <sup>85</sup>Kr, etc.) have been used to understand groundwater dynamics and pollution (Kendall and McDonnell 1998; Cook and Herczeg 2000). Evaporation process causing elevated levels of F<sup>-</sup> in groundwater also leads to enriched isotopic composition, while rock weathering contributing to high F<sup>-</sup> in groundwater does not impact its stable isotopic composition.

The stable isotopic composition of the groundwater varies from -5.3 to -2.3 ‰ for δ<sup>18</sup>O and -33.8 to 18.3 ‰ for δ<sup>2</sup>H. From the stable isotopic systematic, it can be inferred that central parts of the study region show relatively depleted isotopic composition, δ<sup>18</sup>O -5.3 to -4.0 ‰ (TG-2,3,4,6,7 and 8) and the values get enriched down the groundwater flow line, δ<sup>18</sup>O -4.0 to -2.2 ‰ (TG-12, 18, 19 and 24). Quarry contribution is noticed at TG-1, 21 and 23, while Brahmani river shows minor influence on TG-29, whereas Nandira Nala influences TG-19 and 24. Most of the groundwaters from other locations show no or little influence from the surface water bodies. Low F<sup>-</sup>/Cl<sup>-</sup> ratio samples also show depleted isotopic composition compared to high F<sup>-</sup>/Cl<sup>-</sup> ratio samples (Fig. 2b) further confirming the impact of evaporation on F<sup>-</sup> distribution in groundwater of this area. A plot of δ<sup>2</sup>H versus δ<sup>18</sup>O composition of the water samples is shown in Fig. 6. Global meteoric water line (GMWL) and local meteoric water line (LMWL) constructed based on the local rain water were also shown for comparison. It is observed that the stable isotopic data of the water samples fall along with the LMWL. There is no clear differentiation between groundwater affected by evapotranspiration and/or rock weathering (Fig. 6). However, from the plot, it can be

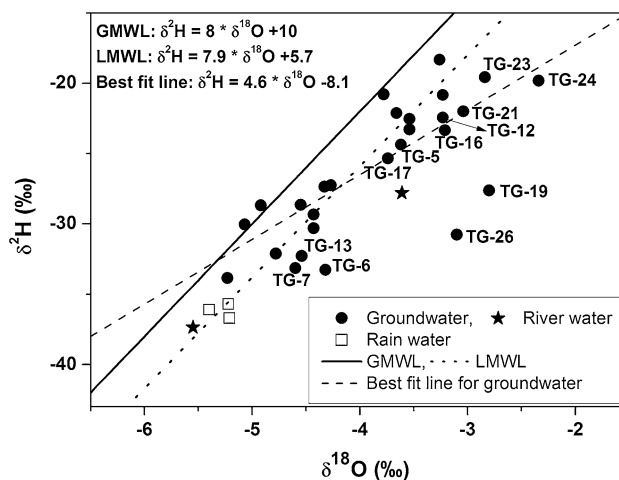


**Fig. 6** Scatter plot δ<sup>2</sup>H versus δ<sup>18</sup>O values of water samples

seen that the groundwater data fall on the best fit line with a slope of 4.8, indicating an overall evaporation effect. Two groundwater samples show highly enriched values (TG-19 and 26), which could be due to evaporated surface water contribution. Rainwater samples show maximum depletion in stable isotopic values among all samples, while river samples show both depleted and enriched isotope composition.

A few water samples were measured for environmental tritium and the values range from 1.7 to 3.4 T.U. Rainwater samples show values in the range of 3–5 TU. From the tritium data, it can be inferred that all the groundwaters are recharged by modern precipitation (<50 years). Only two samples show tritium values less than 2 TU indicating longer residence times for these groundwaters. In general it is observed that samples containing high fluoride contain low tritium (Fig. 7). This suggests that long residence time of groundwater is a critical parameter controlling the water–rock interaction and accumulation of fluoride in groundwater.

### Fluoride release mechanism

Generally fluoride level in the groundwater largely depends on the availability of F-bearing minerals and their leaching from the rock. The common fluoride minerals present in granitic rocks are fluorite, micas (biotite) and hornblende (Jacks et al. 2005). Another common mineral is apatite in which  $F^-$  may replace  $OH^-$  ions to a variable extent and depending upon the alkaline nature of groundwater the  $F^-$  may be released back into groundwater. XRD studies in this region reported minerals such as amphiboles, plagioclase, chlorites, zeolites and smectite (Bhattacharya et al. 2002). Mineralogy of the study area indicates the presence

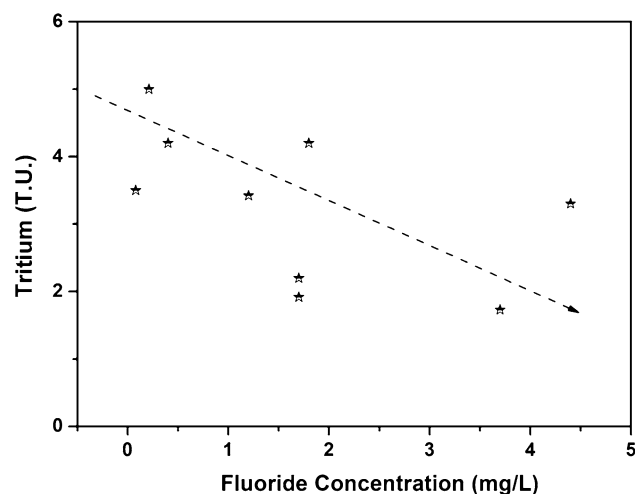


**Fig. 7** Plot depicting the relationship between  $^3H$  content and  $F^-$  concentration in water samples

of chert, quartzite, hornblende and carbonate minerals (Dasgupta 2006; Gawande et al. 2002). It is reported that fluoride concentration in granitic and carbonate rocks is about 0.1 and 0.03 %, respectively (Jeffery 1970), while high abundances are reported in hornblende and biotite, 2.9 and 1.1 %, respectively (Jagadeshan et al. 2015). In addition to the geochemical reactions between groundwater and fluoride minerals, evaporation is another important factor controlling the distribution of fluoride groundwater.

Natural mechanisms controlling the chemistry of the groundwater including water–rock interaction, evaporation and atmospheric precipitation, and these processes are commonly illustrated by Gibbs (1970). The TDS was plotted against molar ratios of  $Na^+/(Na^++Ca^{2+})$  for cations and  $Cl^-/(Cl^-+HCO_3^-)$  for anions (Fig. 8a, b). It was found that majority of the samples are clustered in a zone dominated by rock–water interaction with the influence of evaporation. Contribution of rock weathering is further confirmed by the content of  $Cl^-$  with reference to other anions of the groundwater ( $Cl^-/\sum$  anions ratio). This ratio <0.8 signifies contribution of rock weathering towards groundwater chemistry (Hounslow 1995). This ratio in groundwater samples of this area was found to vary from 0.06 to 0.78 (Table 4), and all samples show this ratio <0.8, indicating that rock weathering is a dominant process in this region.

The fluoride levels in groundwater are proportional to the degree of water–rock interactions. During chemical weathering, many minerals along with chemical species release into groundwater as the parent rock dissociates and disintegrates. Fluoride is lost during weathering at approximately same rate as other elements from the minerals. Hence, a correlation between lithogenic  $Na^+$  and  $F^-$  is a good indicator to identify the weathering contribution

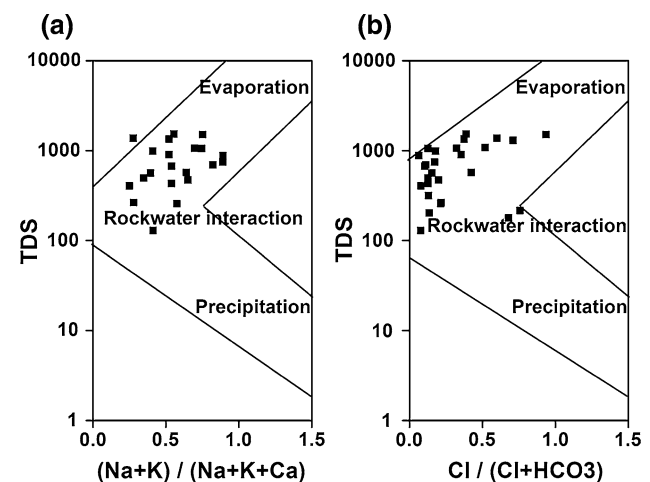


**Fig. 8** Plots of TDS versus **a**  $Na^++K^+/(Na^++K^++Ca^{2+})$  and **b**  $Cl^-/(Cl^-+HCO_3^-)$ , which illustrate the dominant processes that control the chemistry of groundwater

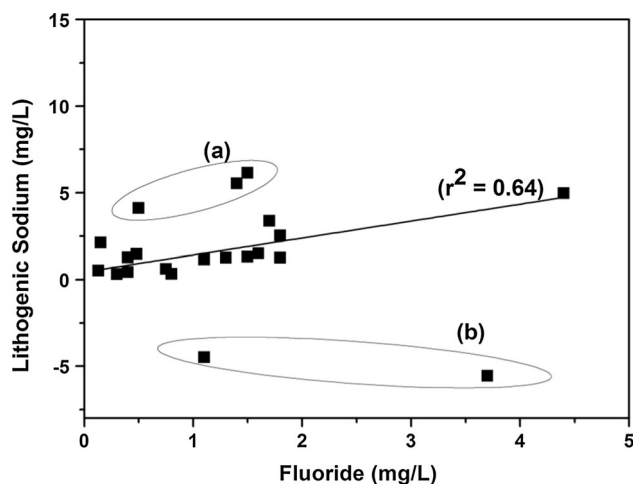


**Fig. 9** Plots of lithogenic sodium (LNa) versus  $F^-$  concentration in groundwater samples

of  $F^-$  to groundwater. Lithogenic  $Na^+$  (LNa) is the net  $Na^+$  concentration acquired by groundwater from chemical weathering of rocks only (Keesari et al. 2007; Ramesham and Rajagopalan 1985; Shaji et al. 2007). The value of LNa is calculated on the basis of the chloride ( $Cl^-$ ) concentration using the following formula;

$$LNa = [Na^+] - [Cl^-] \tag{8}$$

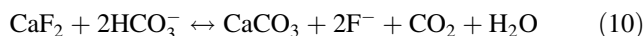
All concentrations are expressed in milliequivalents per liter. In Fig. 9, groundwater samples show a positive correlation [ $r^2 = 0.64$ , excluding groups (a) and (b)] pointing that the  $F^-$  in the groundwater is mainly attributed to rock weathering process. Group (a) samples falling above the line (TG-11, 13 and 23) indicate additional sources of sodium or removal of fluoride by its inclusion in concretions (Jacks et al. 2005). Group (b) samples (TG-19 and 28) falling below the line indicate additional sources of fluoride in groundwater, which is already observed from

stable isotopic composition (“Environmental isotopic characteristics” section).

The solubility of fluorite is low ( $K_{sp} = 3.9 \times 10^{-9}$ ), and the chemical equilibrium reaction for its dissolution can be written as follows;



Since the solubility of fluorite is low, it precipitates even at very low concentrations of  $F^-$ , which is evident by the presence of fluorite secondary precipitates (Jacks et al. 1993). The solubility of fluorite further decreases in the presence of  $Ca^{2+}$  and  $SO_4^{2-}$ . A negative correlation was commonly observed between  $F^-$  and  $Ca^{2+}$  in high  $F^-$  groundwaters (Handa 1975; Jacks et al. 2005; Keesari et al. 2007) indicating calcite precipitation as the driving force for enhanced fluorite solubility and hence high  $F^-$  concentration in groundwater. In the present study, no correlation was observed between  $Ca^{2+}$  and  $F^-$  ( $r = 0.04$ , Table 5), but chemical facies of all the groundwaters containing high  $F^-$  concentration invariably showed  $HCO_3^-$  dominance (except TG-19, which is  $Cl^-$  dominant). It indicates that presence of  $HCO_3^-$  facilitates in fluoride release from the minerals. The chemical reaction can be written as follows:



Many researchers reported a positive correlation between  $F^-$  and  $HCO_3^-$  (Jacks et al. 2005; Keesari et al. 2007) but on the contrary, no systematic correlation was found between  $F^-$  and  $HCO_3^-$  concentrations in the present study ( $r = 0.13$ , Table 5). This implies that other additional factors/processes are responsible for fluoride release into groundwaters and might have masked the negative correlation between  $F^-$  and  $Ca^{2+}$  concentrations and positive correlation between  $F^-$  and  $HCO_3^-$  concentration, which were commonly observed features. Among

**Table 5** Correlation matrix depicting the inter-ion relationship of water samples

	pH	EC	TDS	$Na^+$	$K^+$	$Mg^{2+}$	$Ca^{2+}$	$F^-$	$Cl^-$	$NO_3^-$	$SO_4^{2-}$	$HCO_3^-$
pH	1											
EC	0.118	1										
TDS	0.119	1	1									
$Na^+$	0.144	0.637	0.636	1								
$K^+$	0.132	0.224	0.227	0.075	1							
$Mg^{2+}$	0.111	0.588	0.588	0.725	0.287	1						
$Ca^{2+}$	0.155	0.47	0.47	0.437	0.404	0.69	1					
$F^-$	-0.013	0.396	0.395	0.583	-0.206	0.349	0.004	1				
$Cl^-$	-0.301	0.518	0.518	0.535	0.001	0.603	0.264	0.526	1			
$NO_3^-$	0.177	0.278	0.277	0.258	-0.011	0.566	0.586	-0.013	0.33	1		
$SO_4^{2-}$	-0.06	0.393	0.392	0.442	0.001	0.466	0.286	0.304	0.796	0.583	1	
$HCO_3^-$	0.512	0.311	0.311	0.378	0.033	0.217	0.363	0.126	-0.2	0.281	0.132	1

other inter ionic correlation, strong positive correlations were noted among (a) TDS with  $\text{Na}^+$ ,  $\text{Mg}^{2+}$  and  $\text{Cl}^-$ , (b) Na with  $\text{Mg}^{2+}$ ,  $\text{F}^-$  and  $\text{Cl}^-$ , (c)  $\text{Mg}^{2+}$  with  $\text{Ca}^{2+}$ ,  $\text{Cl}^-$  and  $\text{NO}_3^-$ . All these correlations hint at the contribution of rock weathering, ion exchange, anthropogenic activities toward  $\text{F}^-$  distribution in groundwater. There is no significant strong positive or negative correlation between fluoride and other ions except  $\text{Na}^+$  and  $\text{Cl}^-$  ( $r > 0.5$ ). This indicates that  $\text{F}^-$  is not contributed by a single geochemical process but a combination of processes. Similarly,  $\text{F}^-$  and pH showed no correlation, indicating anion exchange might not be the dominant process for fluoride release into groundwater.

Instead of  $\text{F}^-$  concentration,  $\text{F}^-/\text{Cl}^-$  ratio was used in this study to evaluate the role of evapotranspiration and weathering processes on the observed trends among  $\text{F}^-$ ,  $\text{Ca}^{2+}$  and  $\text{HCO}_3^-$  concentrations. From the correlation between  $\text{F}^-/\text{Cl}^-$  molar ratio and  $\text{Ca}^{2+}$ , it can be inferred that low  $\text{F}^-/\text{Cl}^-$  waters are generally high in  $\text{Ca}^{2+}$ , while the high  $\text{F}^-/\text{Cl}^-$  waters are low in  $\text{Ca}^{2+}$  (Fig. 10a, dashed trend line). In the case of correlation between  $\text{F}^-/\text{Cl}^-$  and  $\text{HCO}_3^-$  concentration, a few samples with  $\text{F}^-/\text{Cl}^-$  samples fall parallel to  $\text{HCO}_3^-$  axis (Fig. 10b, shown in box), indicating evapotranspiration leading to high  $\text{HCO}_3^-$  concentration while keeping the  $\text{F}^-/\text{Cl}^-$  ratio constant. Rest of the samples show an increase in  $\text{HCO}_3^-$  concentration with corresponding increase in  $\text{F}^-/\text{Cl}^-$  ratio (Fig. 10b, solid trend line), indicating that alkalinity drives the fluoride leaching into groundwater. These observations are in good agreement with the inferences obtained from earlier discussion (“Geochemical evolution of groundwaters” and “Environmental isotopic characteristics” sections).

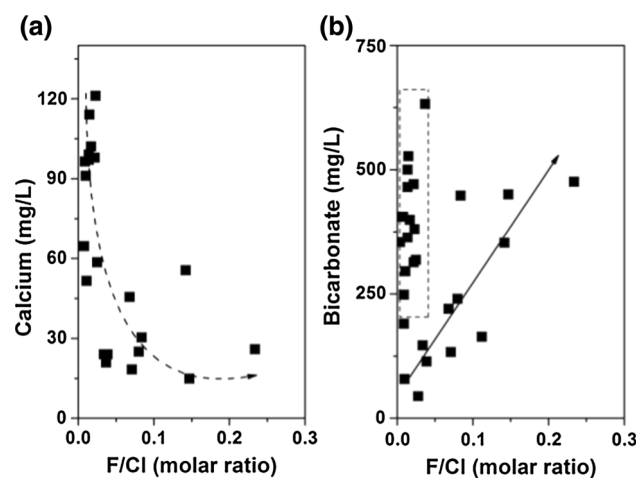


**Fig. 10** Correlation of  $\text{F}^-/\text{Cl}^-$  molar ratio with **a**  $\text{Ca}^{2+}$  and **b**  $\text{HCO}_3^-$  concentrations. Dotted and solid lines indicate eye guide to the sample data

Saturation indices for fluorite and other minerals (carbonate and sulfate) were determined in order to investigate the thermodynamic controls on fluoride concentration in water and also to calculate approximately the levels to which the groundwater has equilibrated with these phases within the rock matrix. Saturation index (SI) of groundwater for a particular mineral is calculated as

$$\text{SI} = -\log \frac{\text{IAP}}{K_{\text{sp}}} \quad (11)$$

where IAP is the ion activity product and  $K_{\text{sp}}$  is the mineral solubility product. At saturation, the saturation index equals zero, whereas positive and negative values indicate supersaturation and undersaturation, respectively. Saturation indices for minerals like calcite, dolomite, gypsum and fluorite were calculated using WATEQ4F program (Plummer et al. 1976) and is given in Table 4.

SI values confirm that most of the groundwaters are unsaturated w.r.t. fluorite and gypsum, whereas samples show wide variation in dolomite and calcite solubility. Plot of  $\text{SI}_{\text{fluorite}}$  versus  $\text{SI}_{\text{minerals}}$  indicates that most of the groundwater sample data fall in dolomite and calcite saturated zone (Fig. 11), indicating effective interaction between groundwater and carbonate minerals. A few samples show unsaturation with respect to dolomite and calcite, which can be attributed to slightly acidic nature of these waters (pH 6–6.5). In addition, faster circulation of groundwater which reduces effective water–rock interaction also might be a cause for this unsaturation. Very few samples show supersaturation especially w.r.t. dolomite, which can be caused due to incongruent dissolution, common ion effect, evaporation, rapid increase in temperature and  $\text{CO}_2$  exsolution (Langmuir 1997). In the case of gypsum, all the samples show unsaturation, while most of the samples show unsaturation w.r.t. magnesite, which

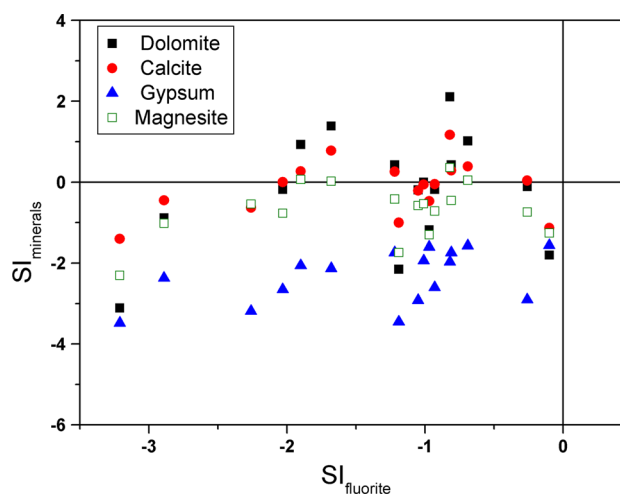


**Fig. 11**  $\text{SI}_{\text{fluorite}}$  versus  $\text{SI}_{\text{minerals}}$  of groundwater samples

could be due to higher solubility of magnesium minerals compared to calcium minerals and also low concentration of  $Mg^{2+}$  in groundwater (mean: 32 mg/L). SI values of fluorite in all the groundwater show unsaturation indicating that fluorite dissolution controls the fluoride solubility in groundwater (Fig. 11; Table 4). From the SI values it can be observed that few samples show super saturation with calcite and unsaturation with fluorite. These characteristics infer that calcite precipitation is the driving force for fluorite dissolution, in spite of low solubility of fluorite.

**Statistical analysis**

Multivariate statistical treatment of hydrochemical data is employed in this study to corroborate the findings obtained from geochemical and environmental isotopic data. Principal component method is used for parameter estimation and transforming the observed independent variables into an orthogonal set of variables called principal components. The factor analysis for samples is carried out using SPSS statistical software, and the highest four varimax rotated factor loadings are given in Table 6. The four maximum factors contribute to 78 % of the Total Data Variability (TDV). The first factor is represented by EC, TDS and major ions ( $Na^+$ ,  $Mg^{2+}$ ,  $F^-$  and  $Cl^-$ ) with a TDV of 41 %, clearly indicating the contribution of rock weathering (Brindha et al. 2016). This indicates that the dominant process for the elevated fluoride levels in these groundwaters is contribution from rock weathering. This factor also confirms that high sodicity and high TDS facilitate release of  $F^-$  in groundwater of this area. The second factor is represented by  $NO_3^-$  and  $SO_4^{2-}$  with a TDV of 15 %, indicating the impact of atmospheric sources. Different gasses emanating from industries and vehicles lead to high concentration of these ions, which can be brought into groundwater through precipitation.

**Table 6** Factor analysis of groundwater data, Talchir area

	1	2	3	4
pH	-0.103	0.228	0.055	0.731
EC	0.822	-0.061	0.278	0.22
TDS	0.821	-0.062	0.279	0.22
$Na^+$	0.805	0.115	0.174	0.181
$K^+$	0.024	-0.326	0.71	0.043
$Mg^{2+}$	0.629	0.335	0.563	0.002
$Ca^{2+}$	0.284	0.284	0.832	0.141
$F^-$	0.759	0.027	-0.359	0.106
$Cl^-$	0.778	0.329	0.045	-0.467
$NO_3^-$	0.186	0.768	0.393	0.105
$SO_4^{2-}$	0.574	0.575	0.054	-0.182
$HCO_3^-$	0.167	0.16	0.186	0.836

Rain water composition of this region also supports this inference. Negative score for  $K^+$  indicates ion exchange or uptake of  $K^+$  by plants. Third factor is represented  $K^+$  and  $Ca^{2+}$  with a TDV of 12 %. This factor indicates contribution from carbonate, feldspar minerals and ion exchange. The negative score by  $F^-$  indicates adsorption of  $F^-$  into calcite concretions. Fourth factor is represented by pH and  $HCO_3^-$  ion with a TDV of 10 % indicating control of pH on inorganic carbon distribution.

**Summary and conclusions**

Groundwater chemistry and its suitability to drinking and causes for fluoride occurrence were evaluated in the Talcher area, Odisha. This study is significant as the water resources are being endangered by the mining and other industrial activities in this region. Among different hydrochemical parameters except  $F^-$  other parameters are well within the drinking water permissible limits. Results suggest that sodium and calcium are major cations, whereas bicarbonate and chloride are major anions. The fluoride concentrations in the study are found in the range of 0.1 to 4.4 mg/L. From the  $F^-$  concentration data, it is evident that about 48 % of the groundwater samples can lead to detrimental effects upon consumption for drinking purposes. Geochemical characterization of groundwater shows that the chemical facies of water samples were found to be closely linked to the lithology of the study area. Two geochemical pathways have been identified for the enrichment of fluoride in groundwater, viz., rock weathering and evapotranspiration. Rock weathering is found to be the dominant process controlling the fluoride distribution followed by evapotranspiration. A positive correlation was observed between  $F^-$  and LNa,  $Cl^-$  to sum of anions ratio, Gibbs plot and statistical analysis, which infer that groundwater chemistry is influenced by rock weathering and ion exchange followed by precipitation of minerals due to evapotranspiration.

Environmental isotope data indicates that the groundwater isotopic signatures are not different for high and low fluoride locations. There is no clear differentiation between groundwater sampled near or away from the mining sites indicating that mining might not be the only source of fluoride in groundwater as opined by the researchers. Since the geology of the area is dominated by minerals derived from granitic rocks which have abundant fluoride content and the groundwater being under unsaturated condition with respect to fluorite mineral, higher fluoride contamination levels in groundwater can be expected.

**Acknowledgments** Authors sincerely thank Talcher Power Plant authorities for their support during this work. Dr. K.L. Ramakumar,

Director, RC & I Group, Head, Isotope Applications Division, B.A.R.C. is gratefully acknowledged. Thanks are also due to Mr. T. B. Joseph, former colleague of Isotope Hydrology section for the help rendered during sample collection and Dr. S. Chidambaram, Prof. Dept. Earth Sciences, Annamalai University, Tamil Nadu, for providing geochemical model output and figures.

## References

- Ando M, Tadano M, Yamamoto S (2001) Health effects of fluoride pollution caused by coal burning. *Sci Total Environ* 271:107–116
- Ayoob S, Gupta AK (2006) Fluoride in drinking water: a review on the status and stress effects. *Crit Rev Environ Sci Technol* 36(6):433–487
- Battaleb-Looie S, Moore F, Jafari H, Jacks G, Ozsvath D (2012a) Hydrogeochemical evolution of groundwaters with excess fluoride concentrations from Dashtestan, South of Iran. *Environ Earth Sci* 67(4):1173–1182
- Battaleb-Looie S, Moore F, Jacks G, Ketabdari MR (2012b) Geological sources of fluoride and acceptable intake of fluoride in an endemic fluorosis area, southern Iran. *Environ Geochem Health* 34:641–650
- Battaleb-Looie S, Moore F, Malde MK, Jacks G (2013) Fluoride in groundwater, dates and wheat: estimated exposure dose in the population of Bushehr, Iran. *J Food Compos Anal* 29(2):94–99
- Bhattacharya SK, Prosenjit G, Chakrabarti A (2002) Isotopic analysis of Permo-Carboniferous Talchir sediments from East-Central India: signature of glacial melt-water lakes. *Chem Geol* 188:261–274
- Brindha K, Jagadesh G, Kalpana L, Elango L (2016) Fluoride in weathered rock aquifers of southern India: managed aquifer recharge for mitigation. *Environ Sci Pollut Res*. doi:10.1007/s1356-016-6069-7
- Chae GT, Yun ST, Bernhard M, Kim KH, Kim SY, Kwon JS (2007) Fluorine geochemistry in bedrock groundwater of South Korea. *Sci Total Environ* 385(1):272–283
- Chandrawanshi CK, Patel KS (1999) Fluoride deposition in central India. *Environ Monit Assess* 55:251–265
- Chatterjee A, Roy RK, Ghosh UC, Pramanik T, Kabi SP, Biswas K (2008) Fluoride in water in parts of Raniganj coalfield, West Bengal. *Curr Sci* 94:309–311
- Chaurasia S, Mishra SK (2007) Fluoride contamination in Rain water of Singrauli region. *IJEP* 10:923–928
- Chebotarev II (1955) Metamorphism of natural waters in the crust of weathering. *Geochim Cosmochim Acta* 8:22–48
- Clark I, Fritz P (1997) Environmental isotopes in hydrogeology. Lewis Publ, Boca Raton
- Cook Peter G, Herczeg Andrew L (2000) Environmental tracers in subsurface hydrology. Kluwer Academic Publishers, Dordrecht
- Coplen TB (1996) New guidelines for reporting stable hydrogen, carbon and oxygen isotope-ratio data. *Geochim Cosmochim Acta* 60:3359–3360
- Craig H, Gordon LI, Horibe Y (1963) Isotope exchange effects in the evaporation of water. 1. Low temperature experimental results. *J Geophys Res* 68:5079
- Das DK, Burman GK, Kidwai AL (1981) Chemical composition of monsoon rainwater over Bhopal, Madhya Pradesh during 1977 and 1978. *Mausam* 32:221–228
- Dasgupta P (2006) International Gondwana symposium, vol II. Hindustan Pub. Co., Delhi, pp 617–625
- Datta PS, Deb DL, Tyagi SK (1996) Stable isotope ( $^{18}\text{O}$ ) investigations on the processes controlling fluoride contamination of groundwater. *J Contam Hydrol* 24:85–96
- David MD, Gentry LE (2000) Anthropogenic inputs of nitrogen and phosphorus and riverine export for Illinois, USA. *J Environ Qual* 29:494–508
- Deshmukh AN, Shah KC, Appulingam S (1995) Coal Ash: a source of fluoride contamination, a case study of Koradi thermal power station, District Nagpur, Maharashtra. *Gondwana Geol Mag* 9:21–29
- Dhadse SK, Bhagia LJ (2008) Fly ash characterization and utilization and government initiatives in India—a review. *J Sci Ind Res* 67:11–18
- Dhakate R, Rao TR (2010) Assessment of groundwater quality in Talcher Coalfield Area, Orissa, India. *J Earth Sci Eng* 3:43–55
- Dhakate R, Mahesh J, Sankaran S, Gurunadha Rao VVS (2013) Multivariate statistical analysis for assessment of groundwater quality in Talcher Coalfield Area, Odisha. *J Geol Soc India* 82:403–412
- Dissanayake CB (1991) The fluoride problem in the ground water of Sri Lanka—environmental management and health. *Int J Environ Stud* 38:2–3
- Epstein S, Mayeda T (1953) Variation of  $^{18}\text{O}$  contents of water from natural sources. *Geochim Cosmochim Acta* 4:213–224
- Farooqi A, Masuda H, Kusakabe M, Naseem M, Firdous N (2007) Distribution of highly arsenic and fluoride contaminated groundwater from east Punjab, Pakistan, and the controlling role of anthropogenic pollutants in the natural hydrological cycle. *Geochem J* 4(1):213–234
- Frencken JE (1992) Endemic fluorosis in developing countries, causes, effects and possible solutions. Publ. No. 91.082, NIPGTNO, Leiden
- Gawande RR, Srivatsava AK, Jeyaram A (2002) Geological, geomorphological, hydrogeological and land use/land cover studies around kamthi area, Nagpur district, Maharashtra using remote sensing techniques. *J Ind Soc Remote Sens* 30(1):95–104
- Gibbs RJ (1970) Mechanisms controlling world water chemistry. *Science* 17:1088–1090
- Guo Q, Wang Y, Ma T, Ma R (2007) Geochemical processes controlling the elevated fluoride concentrations in groundwaters of the Taiyuan Basin, Northern China. *J Geochem Explor* 93:1–12
- Handa BK (1975) Geochemistry and genesis of fluoride containing ground waters in India. *Ground Water* 13:275–281
- Hem JD (1985) Study and interpretations of the chemical characteristics of natural water. U.S. Geological Survey Water Supply Paper, U.S. Geological Survey, Alexandria, Virginia, USA
- Horita J, Ueda A, Mizukami K, Takatori I (1989) Automatic  $\delta\text{D}$  and  $\delta^{18}\text{O}$  analyses of multi-water samples using  $\text{H}_2$ - and  $\text{CO}_2$ -water equilibration methods with a common equilibration set-up. *Int J Radiat Appl Instrum Part A Appl Radiat Isot* 40:801–805
- Hounslow AW (1995) Water quality data-analysis and interpretation. Lewis Publishers, CRC Press, Boca Raton
- Jacks G, Rajagopalan K, Alveteg T, Jonsson M (1993) Genesis of high-F groundwaters, Southern India. *Appl Geochem Suppl* 2:241–244
- Jacks G, Bhattacharya P, Chaudhary V, Singh KP (2005) Controls on the genesis of some high-fluoride groundwaters in India. *Appl Geochem* 20:221–228
- Jagadesh G, Kalpana L, Elango L (2015) Major ion signatures for identification of geochemical reactions responsible for release of fluoride from geogenic sources to groundwater and associated risk in Vaniyar River basin, Dharmapuri district, Tamil Nadu, India. *Environ Earth Sci* 74:2439–2450
- Jankowski J, Acworth RI, Shekarfroush S (1998) Reverse ion exchange in a deeply weathered porphyritic dacite fractured aquifer system, Yass, New South Wales, Australia. In: Arehart GB, Hulston JR (eds) Proceedings of the 9th international



- symposium, water–rock interaction. Balkema, Rotterdam, pp 243–246
- Jeffery PG (1970) Chemical methods or rock analysis, 1st edn. Pergamon Press, New York
- Keesari T, Shivanna K, Jalihal AA (2007) Isotope hydrochemical approach to understand fluoride release into groundwaters of Iikal area, Bagalkot District, Karnataka, India. *Hydrogeol J* 15:589–598
- Kendall C, McDonnell JJ (1998) Isotope tracers in catchment hydrology. Elsevier Science, Amsterdam
- Kern ML, Vieiro AP, Machado G (2008) The fluoride in the groundwater of Guarani Aquifer System: the origin associated with black shales of Parana Basin. *Environ Geol* 55(6):1219–1233
- Kundu N, Panigrahi MK, Tripathy S, Munshi S, Powell MA, Hart BR (2001) Geochemical appraisal of fluoride contamination of groundwater in the Nayagarh District of Orissa, Indian. *Environ Geol* 41(3):451–460
- Langmuir D (1997) Aqueous environmental geochemistry. Prentice-Hal, New Jersey
- Manjrekar VD, Choudhary VN, Goutam KVV (1998) Coal. Geology and mineral resources of Orissa. Society of Geoscientists and Allied Technologists, Bhubaneswar, pp 179–203
- Moghaddam AA, Fijani E (2009) Hydrogeologic framework of the Maku area basalts, Northwestern Iran. *Hydrogeol J* 17(4):949–959
- Moharana JK, Nanda PM, Garnaik BK (2013) Eutrofication due to industrialization in Angul-Talcher industrial complex of Odisha. *Int J Sci Environ Technol* 2:20–27
- Nair AR (1983) Possibilities of liquid scintillation counting for tritium and radiocarbon measurements in natural water. In: Proceeding of the workshop on isotope hydrology. Bhabha Atomic Research Centre, Mumbai, pp 41–56
- Nanda PM, Garnaik BK, Panda Sunakar (2011) Studies on fluoride pollution in ground water of Angul-Talcher industrial complex of Odisha, India. *Asian J Chem Environ Res* 4:13–16
- Nelson TS (2000) A simple, practical methodology for routine VSMOW/SLAP normalization of water samples by continuous flow methods. *Rapid Commun Mass Spectrom* 14:1044–1046
- Ohsumi T, Fujino H (1986) Isotopic exchange technique for preparation of hydrogen gas in mass spectrometric D/H analysis of natural waters. *Anal Sci* 2:489–490
- Panda RB, Panda Gitarani, Pradhan D (2010) Ground water quality in Talcher industrial complex, Odisha, India. *Pollut Res* 29(3):539–543
- Pillai KS, Stanley VA (2002) Implications of fluoride—an endless uncertainty. *J Environ Biol* 23:81–87
- Plummer LN, Jones BF, Truesdell AH (1976) WATEQF—a Fortran IV version of WATEQ, a computer program for calculating chemical equilibrium of natural waters. US Geol Surv Water Resources Investigations Report, 76-13
- Praharaj T, Tripathy S, Powell MA, Hart BR (2003) Geochemical studies to delineate topsoil contamination around an ash pond of a coal-based thermal power plant in India. *Environ Geol* 45:86–97
- Rai D (1987) Inorganic and organic constituents in fossil fuel combustion residues research project, vol 2. Electric Power Research Institute, Columbus, Ohio, USA, pp 2485–2488
- Ramesham V, Rajagopalan KJ (1985) Fluoride ingestion into the natural water of hard rock areas, Peninsular India. *J Geol Soc India* 26:125–132
- Rango T, Bianchini G, Beccaluva L, Ayenew T, Colombani N (2009) Hydrogeochemical study in the main Ethiopian rift: new insights to source and enrichment mechanism of fluoride. *Environ Geol* 58:109–118
- Reza R, Singh Gurdeep (2010) Assessment of ground water quality status by using water quality index method in Orissa, India. *World Appl Sci J* 9:1392–1397
- Reza R, Singh Gurdeep (2013) Groundwater quality status with respect to fluoride contamination in industrial area of Angul district, Orissa, India. *Ind J Sci Res Technol* 1(3):54–61
- Reza R, Jain MK, Singh G (2009) Pre and post monsoon variation of heavy metals concentration in ground water of Angul-Talcher Region of Orissa, India. *Nat Sci* 7(6):52–56
- Saether OM, Andreassen BTh, Semb A (1995) Amounts and sources of fluoride in precipitation over southern Norway. *Atmos Environ* 29:1785–1793
- Sahu BK, Panda RB, Sinha BK (1991) Water quality index of the river Brahmani at Rourkele industrial complex. *J Ecotoxocol Environ Monit* 3:169–175
- Satsangi GR, Lakhani A, Khare P, Singh SP, Kumar SS, Srivatsava SS (1998) Composition of rainwater at a semiarid rural site in India. *Atmos Environ* 32:3783–3793
- Satsangi GR, Lakhani A, Khare P, Singh SP, Kumar SS, Srivatsava SS (2002) Measurement of major ion concentrations in settled coarse particles and aerosols at a semiarid rural site in India. *Environ Int* 28:1–7
- Schoeller H (1967) Qualitative evaluation of groundwater resource. Methods and techniques of groundwater investigation and development. *Water Res* 33:44–52
- Shaji E, Bindu Viju J, Thambi DS (2007) High fluoride in groundwater of Palghat district, Kerala. *Curr Sci* 92:240–245
- Singh SP, Khare P, Satsangi GR, Lakhani A, Kumar SS, Srivatsava SS (2001) Rainwater composition at a regional representative site of a semiarid region of India. *Water Air Soil Pollut* 127:93–108
- Singh CK, Kumari R, Singh N, Mallick F, Mukherjee S (2013) Fluoride enrichment in aquifers of the Thar Desert: controlling factors and its geochemical modeling. *Hydrol Process* 27:2462–2474
- Subba Rao N (2011) High-fluoride groundwater. *Environ Monit Assess* 176:637–645
- Subba Rao N, Subrahmanyam A, Babu Rao G (2013) Fluoride-bearing groundwater in Gummanampadu sub-basin, Guntur district, Andhra Pradesh, India. *Environ Earth Sci* 70:575–586
- Tiwary RK, Dhakate R, Sinha A, Singh VS (2009) Evaluation of impact of mining on groundwater resources in Talcher Coalfield, India. *Int J Earth Sci Eng* 2:238–252
- Tripathi SD, Aravindakshan PK, Ayyappan S, Jena JK, Muduli HK, Suresh C, Pani KC (2000) New high in crop production in India through intensive polyculture. *J Aquac Trop* 15:119–128
- UNICEF (1999) State of the art report on the extent of fluoride in drinking water and the resulting endemicity in India. Report by Fluorosis and Rural Development Foundation for UNICEF, New Delhi
- Wang G, Cheng G (2001) Fluoride distribution in water and the governing factors of environment in arid north-west China. *J Arid Environ* 49:601–614
- Wang L, Huang J (1995) Outline of control practice of endemic fluorosis in China. *Soc Sci Med* 41(8):1191–1195
- Wang Y, Wei FS (1995) Chemistry of elements in the pedosphere environment. *Environ Scien Press*, Beijing, pp 129–144
- WHO (2011) Guidelines for drinking water quality. WHO, Geneva
- Zuurdeeg BW, Van der Weiden MJJ (1985) Geochemical aspects of European bottled waters. Geothermics, thermal-mineral waters and hydrogeology. Theophrastus Publications S.A., Athens, pp 235–264